Available online at www.sciencedirect.com

ScienceDirect

Procedia Structural Integrity 44 (2023) 1893–1900

Structural Integrity Procedia

www.elsevier.com/locate/procedia

XIX ANIDIS Conference, Seismic Engineering in Italy

Material characterisation for the numerical modelling of a timber-based seismic retrofit for RC buildings

Francesco Smiroldo[a,]*, Giovanni Sommacal[a], Stylianos Kallioras[b], Dionysios Bournas[b], Maurizio Piazza[a], Ivan Giongo[a]

[a]*University of Trento, via Calepina 14, Trento 38122, Italy*
[b]*European Commission, Joint Research Centre, via Enrico Fermi 2749, Ispra 21027, Italy*

Abstract

Over the past decades, the seismic vulnerability assessment and strengthening of existing reinforced concrete buildings with masonry infills have been topics of great interest for engineers worldwide. Often, such buildings have been designed disregarding lateral loads and the influence of masonry infills on the local and global response, resulting in severe structural damage or collapses in earthquakes. In the context of improving the seismic performance of old reinforced concrete framed buildings, this study draws attention to a seismic retrofit scheme based on cross-laminated timber panels. The effectiveness of the proposed retrofit method has been previously investigated by the authors through advanced numerical modelling. This paper presents the results from an experimental campaign comprising a series of strength tests on materials (e.g., diagonal compression tests on wallettes) and connections (e.g., timber-to-timber and timber-to-concrete connections) employed to realise the retrofit scheme in question. These tests were carried out to improve the predictive accuracy of the numerical models in simulating the coupled behaviour of old reinforced concrete elements, masonry infills, and retrofitting materials. The numerical models were further fine-tuned using data from cyclic quasi-static tests on four full-scale single-bay, single-storey frames. The numerical analysis results appear promising, showing that the proposed retrofit scheme considerably improves the seismic behaviour of reinforced concrete framed structures and that the numerical models can simulate the effect of the retrofit interventions accurately.

Keywords: Seismic retrofit; Material testing; Mechanical characterisation; Masonry infill walls; Reinforced concrete (RC) structures; Cross-laminated timber panels; Nonlinear finite element (FE) analysis.

* Corresponding author.
E-mail address: francesco.smiroldo@unitn.it

10.1016/j.prostr.2023.01.242

1. Introduction

Since the second half of the twentieth century, reinforced concrete (RC) framed structures have spread widely around the world to become one of the most common building construction typologies. However, as Crowley et al. (2021) reported, a large part of these buildings was designed and constructed before the introduction of modern seismic codes; consequently, over the past decades, such structures have exhibited substandard earthquake performance, resulting in significant social and economic losses.

Post-earthquake damage surveys have revealed several pathologies of past construction practices, including inadequate transverse reinforcement, poor reinforcement detailing, irregular stiffness distribution, strong-beam-weak-column and soft-storey mechanisms, all exhaustively discussed in studies like Sezen et al. (2003), Ricci et al. (2011), Darmiel et al. (2022). According to Hashemi (2007), one of the most critical factors affecting the seismic vulnerability of RC-framed buildings is the presence of masonry infill walls due to their interaction with the surrounding frame. The local interaction between masonry infills and RC elements can result in considerable damage and undesirable brittle failure of critical RC elements, such as the shear failure of columns, as reported by Verderame (2011) and Gaetani d'Aragona (2018).

This study is part of a broader experimental and analytical research focusing on using a timber-based structural intervention system for the seismic retrofitting of existing RC-framed structures with masonry infill walls. This retrofit technique exploits the excellent structural performance of the cross-laminated timber (CLT) technology. It has been previously introduced by Smiroldo et al. (2020-2021), who proposed the use of CLT panels in two alternative configurations, termed *RC-TP* and *RC-TPext*. In RC-TP, a timber panel is inserted inside the RC frame by substituting the masonry infill, while in RC-TPext, the CLT panel is applied externally to the RC frame without removing the existing infills.

In this paper, the results from a series of mechanical characterisation tests on materials and components are used to update numerical models generated to perform nonlinear static analyses for the assessment of the proposed seismic retrofit configurations. The analysis results are compared with experimental force-displacement responses obtained from cyclic quasi-static tests on (retrofitted and non-retrofitted) full-scale RC frames up to collapse conditions. A detailed analysis of the data and in-depth discussion of the results from those experiments will be presented in the near future.

2. Intervention strategies

This paper provides only a brief overview of the examined strengthening interventions; the reader is referred to Smiroldo et al. (2020-2021) for a detailed description of the two timber-based retrofit schemes.

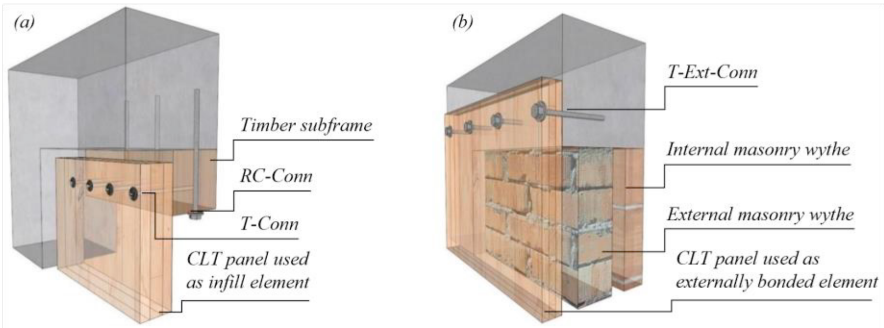

Fig. 1. 3D illustration of the examined intervention schemes: (a) RC-TP; (b) RC-TPext.

The first examined retrofit configuration, termed RC-TP (i.e. Reinforced Concrete frame plus Timber Panels), consists in using CLT panels as infill elements (Fig. 1a). The panels are connected to the existing RC frame through a timber subframe. The connection between a CLT panel and the timber subframe is done with steel screws (T-Conns), while the connection between the timber subframe and the RC frame is realised through steel bars and epoxy (RC-Conns). In the second retrofit scheme, termed RC-TPext (Reinforced Concrete frame plus externally applied Timber

Panels), the CLT panels are attached to the RC frame as externally bonded elements through connections realised with threaded bars reinforced with epoxy; this type of connection is called T-Ext-Conn (Fig. 1b). The masonry infills can be cut at their two vertical edges in a way to separate them from the RC columns and prevent the development of additional shear forces to the RC frame resulting from the diagonal struts formed in the infills.

3. Experimental campaign

The experimental results reported in this paper are part of a broader testing campaign, including four full-scale RC frames (i.e., one non-retrofitted/reference and three retrofitted frames) subjected to cyclic quasi-static in-plane loading of increasing displacement amplitude up to collapse conditions. The reference RC frame included a double wythe masonry infill wall: the internal wythe was made of solid clay bricks, while the external was built with hollow clay blocks. Both masonry wythes were constructed with 10 mm thick mortared head- and bed-joints.

The tests presented here were performed for the mechanical characterisation of materials and connections employed for the seismic retrofitting of the frames. The acquired data were used to update the numerical models developed by Smiroldo et al. (2020-2021) to simulate the force-displacement response of the frames. The design of the RC frame specimens (i.e. geometry and mechanical properties) was carried out in a way to simulate part of a typical RC building from the 70s; for instance, a low-resistance concrete was employed like in Cristofaro et al. (2012).

3.1. Mechanical properties of materials

The compressive strength of the concrete (f_c) used to cast the RC frames was determined through both destructive and non-destructive tests. Destructive compression tests on cores with different aspect ratios (h_c/d_c equal to 1 or 2) were carried out following the norms UNI EN 12504-1 (CEN 2021). Four cores were extracted from a set of $400 \times 400 \times 300$ mm^3 concrete prisms, explicitly cast for sampling concrete. Eight additional samples were extracted from undamaged portions of an RC-framed specimen at the end of the cyclic quasi-static loading tests. Non-destructive rebound tests were performed on the RC prisms before the core sampling, following the standards UNI EN 12504-2 (CEN 2021). Also, tensile tests were performed on longitudinal steel bars and stirrups to estimate their yielding (f_y) and tensile (f_t) strength according to UNI EN 15630-1 (CEN 2019).

Solid bricks and hollow blocks were subjected to compression tests to obtain their compressive strength (denoted f_{sb} and f_{hb}, respectively), following the standard test procedures prescribed in UNI EN 772-1 (CEN 2015). Hollow blocks were subjected to loading applied both parallel and perpendicular to the holes (although they were only laid with the holes oriented horizontally in the infill walls of the full-scale experimental frames). None of the two types of masonry units was tested in the dimensions delivered by the manufacturer; instead, they were cut in smaller prisms to fit in the test apparatus. Specifically, solid bricks were cut to obtain eight 50 mm wide cubes, while hollow blocks were cut perpendicular to the holes to obtain 16 smaller units (eight specimens for testing along each of the two orthogonal directions, i.e., parallel and perpendicular to the holes). Twelve mortar prisms were subjected to three-point bending and compression tests to estimate the flexural ($f_{mor,f}$) and compressive ($f_{mor,c}$) strength of mortar (UNI EN 1015-11; CEN 2019).

Table 1 summarises the average estimates of mechanical material properties obtained from the abovementioned strength tests. Some properties (i.e., the concrete elastic modulus, E_c; the masonry compressive strength, $f_{m,s} - f_{m,w}$; and the masonry Young's modulus, $E_{m,s} - E_{m,w}$) were derived from formulas proposed by Eurocode 2 and Eurocode 6. Here, only the concrete elastic modulus deriving from $f_{c,c2}$ (i.e., the concrete compressive strength obtained from core samples with $h_c/d_c = 2$) is reported ($E_{c,c2}$).

Table 1. Summary of the mechanical properties of the employed materials.

Concrete [MPa]				**Steel reinforcement [MPa]**					
(estimates from rebound tests)	(estimates from compression tests on core samples; E_c derived from formulas proposed by EC2)			(estimates from tensile tests on longitudinal rebars)			(estimates from tensile tests on stirrups)		
	$h_c/d_c = 1$	$h_c/d_c = 2$							
$f_{c,r}$	$f_{c,c,1}$	$f_{c,c,2}$	$E_{c,c,2}$	$f_{l,y}$	$f_{l,t}$	E_l	$f_{s,y}$	$f_{s,t}$	E_s
15.0	10.9	10.0	22000	532	639	206000	562	637	199000

Masonry and components [MPa]								
(from comp. tests on solid bricks)	(from comp. tests on hollow blocks)		(from comp. and bending tests on mortar prisms)		(derived from formulas proposed by EC6; strong masonry wythe, i.e. made of solid clay bricks)		(derived from formulas proposed by EC6; weak masonry wythe, i.e. made of hollow clay blocks)	
f_{sb}	$f_{hb,v}$	$f_{hb,h}$	$f_{mor,f}$	$f_{mor,c}$	$f_{m,s}$	$E_{m,s}$	$f_{m,w}$	$E_{m,w}$
29.9	7.1	4.0	2.1	6.4	10.4	10400	1.6	1600

3.2. Diagonal compression tests on masonry wallettes

The in-plane shear strength (τ_m) of the strong masonry wythe, i.e., the one made of solid clay bricks, was determined through destructive diagonal compression tests on four assemblies of this masonry type. The contribution of the weak wythe (made of hollow blocks) to the in-plane load resistance of the experimental RC frames was considered negligible; as such, no tests on this type of masonry were performed.

Three square 1200 mm wide and 120 mm thick masonry panels (labelled M1, M2 and M3) were subjected to diagonal compression according to the standards for material testing ASTM E519/E519M (ASTM 2020), adopting the experimental setup shown in Fig. 2. A fourth masonry specimen of the same dimensions (labelled M4) was tested in diagonal compression under additional uniform compression perpendicular to the bed-joints to simulate the loading conditions in the experimental full-scale RC frames. This extra compression was equal to approximately 0.16 kN/m and was applied by means of two pairs of pre-tensioned threaded steel bars. In all cases, the diagonal compressive load was applied through a hydraulic jack. The deformation field of each specimen was monitored by two pairs of displacement transducers mounted along the diagonals on both faces of the wallette. Fig. 3 shows the cyclic force-displacement curves (i.e. applied compression load, P, versus absolute deformation, $\delta_{c,mean}$) for all four masonry wallettes.

Wallette M1 Wallette M4

Fig. 2. Diagonal compression tests on masonry wallettes: experimental setup and observed failure modes in specimens M1 and M4.

The three wall specimens tested under standard loading conditions (M1, M2 and M3) exhibited similar behaviour, attaining a mean shear strength equal to 0.14 MPa and a mean ultimate displacement (corresponding to $0.80P_{max}$) equal to 0.95 mm. Wallette M4, which was tested under uniform compression of 0.16 kN/m, attained maximum shear strength of 0.25 MPa and ultimate displacement of 3.84 mm. In addition, wallette M4 exhibited remarkable overstrength after the compression load had dropped to $0.80P_{max}$, reaching a new maximum displacement of 21.8 mm. M1, M2 and M3 mainly exhibited diagonal cracks with shear sliding along the bed-joints, while M4 suffered diffused damage, as shown in Fig. 2.

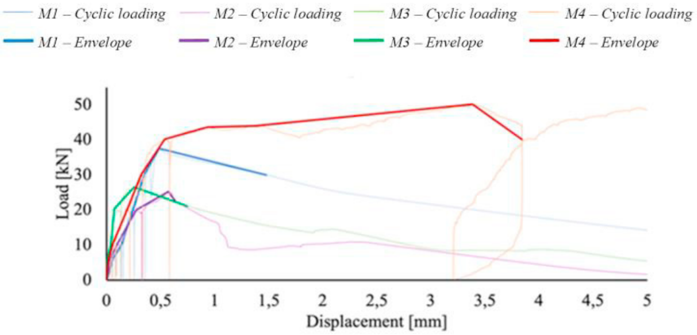

Specimen name	Maximum attained load P_{max} [kN]	Shear strength τ_m [MPa]	Ultimate displacement $\delta_{u,mean}$ [mm]
M1	37.5	0.18	1.48
M2	25.2	0.12	0.64
M3	26.6	0.13	0.74
M4	50.2	0.25	3.84

Fig. 3. Diagonal compression tests on masonry wallettes: comparison of the load-displacement response curves.

3.3. Strength tests on timber-to-timber and timber-to-concrete connections

Strength tests were also performed to determine the mechanical properties and potential failure modes of the various connections involved in the examined seismic retrofit schemes. Specifically, direct shear tests (alternatively called push-out tests) were performed on the T-Conn connection of the retrofit configuration RC-TP (shown in Fig. 1a), and on the T-Ext-Conn bond of the alternative solution, RC-TPext (Fig. 1b). Instead, the connection type RC-Conn (Fig. 1a) was subjected to pull-out tests.

The load resistance and ultimate failure of T-Conn and T-Ext-Conn were explored by performing a series of push-out tests according to the standards UNI EN 26891 (CEN 1991). The tests comprised three T-Conn specimens (explicitly realised for these tests) and two T-Ext-Conn specimens (extracted from undamaged portions of a full-scale RC frame specimen at the end of the cyclic quasi-static tests). Trial testing on a reference specimen was carried out to define the test protocol (i.e., loading rate and unloading-reloading procedure) of the push-out tests. The experimental setups adopted for the two types of tests are illustrated in Fig. 4, while Fig. 5 shows the test results.

Fig. 4. Push-out tests: experimental setup for connection types (a) T-Conn, and (b) T-Ext-Conn.

In order to avoid brittle concrete cone failure in the RC-TP retrofit solution (i.e. extraction of the steel bars from the RC members), the anchors RC-Conn should exhibit some overstrength with respect to the shear capacity of the T-Conn bond. For this reason, Smiroldo et al. (2020) assumed a target overstrength factor equal to 1.3 and pull-out tests were performed on four RC-Conns specimens to verify this overstrength. Specifically, threaded steel bars of diameter 12 mm were inserted by 15 cm into concrete elements taken from undamaged parts of an RC frame specimen; the bond was reinforced with epoxy. Each anchor was subjected to force-controlled semi-cyclic loading of increasing amplitude up to the ultimate extraction of the bar from the concrete block. The mean force causing extraction of a single fastener was equal to 47.1 kN.

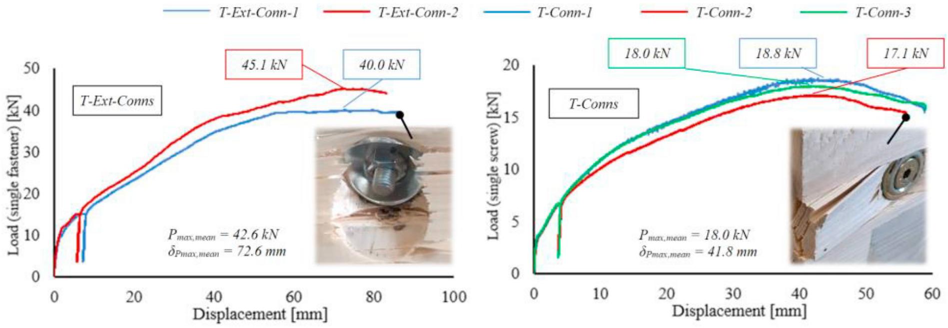

Fig. 5. Push-out tests on connections T-Ext-Conns and T- Conns: comparison of the force-displacement response curves.

4. Numerical simulations

4.1. Modelling updates

The experimental data acquired in the mechanical characterisation tests outlined in previous sections were used to update the mechanical parameters of the numerical models developed by Smiroldo et al. (2020-2021). A 2D illustration of the numerical models is shown in Fig. 6. The most critical updates regarded the definition of the nonlinear links simulating the connections RC-Conns, T-Conns and T-Ext-Conns (see Fig. 1). Specifically, the response curves obtained from the push-out tests (shown in Fig. 5) were used as a reference to define new multilinear shear force-displacement relationships for the springs simulating the connections. Instead, the mean anchor pull-out strength estimated from the pull-out tests was set as a tensile force limit for the RC-Conns.

The data from the cyclic quasi-static tests on the full-scale frames were used to fine-tune further the stiffness and strength degradation of the links from one loading cycle to the other, accounting for the combined effect of shear and tensile forces. In the numerical model of the RC-TPext retrofit configuration, the masonry infill walls were simulated through equivalent diagonal strut elements. The stiffness of the strut element representing the external masonry wythe (i.e., the one not in contact with the RC columns) was reduced by 50% to account for the gap introduced between the RC frame and the wall after cutting the vertical edges of the latter.

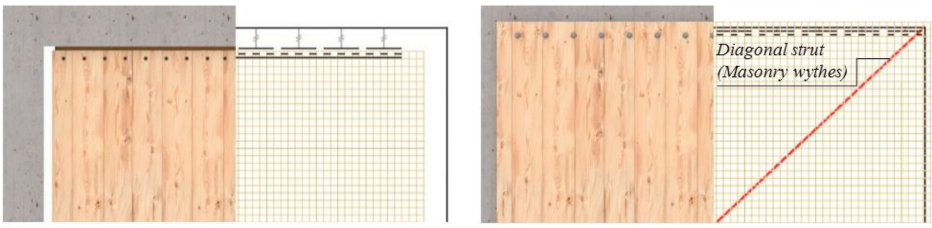

Fig. 6. 2D illustration of the numerical finite element models of the examined retrofit configurations.

4.2. Analysis results

Fig. 7 compares the capacity curves of the experimental frames predicted by the numerical FE models through nonlinear pushover analysis with those obtained from the cyclic quasi-static tests performed in the laboratory. As one can readily observe in Fig. 7, both strengthening interventions resulted in a significantly increased load-bearing capacity with respect to the non-retrofitted masonry-infilled RC frame. Specifically, increases of 120% and 174% were observed for the two frames that benefitted from the RC-TP retrofit scheme, while an increase of 108% was observed in the case of the RC-TPext configuration.

The updated numerical models reproduced the overall experimental force-displacement responses with accuracy. In particular, both in the experiments and the numerical analyses, the reference masonry-infilled frame showed column shear failure due to the additional shear action transmitted by the masonry infill to the RC frame. Instead, the retrofitted frames showed a more ductile behaviour, provided by the progressive yielding/failure of the fasteners and the flexural behaviour of the columns. The reason for which the experimental maximum displacement of specimen RC-TP-Conf.1 was significantly lower than that of RC-TP-Conf.2 is because tests on the first were interrupted due to excessive out-of-plane deflections of the RC frame rather than reaching collapse conditions; until testing was stopped, the numerical model adequately reproduced the experimental response. Overall, the updated numerical models predicted the lateral load-bearing capacity of the retrofitted frames accurately.

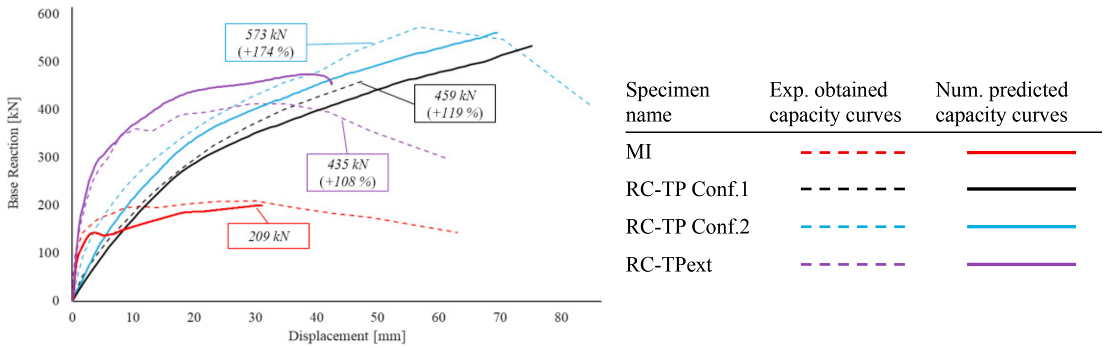

Fig. 7. Comparison between experimental results and predictions by the numerical models: MI, masonry infilled frame; RC-TP Conf.1, retrofit configuration with a 57 mm thick CLT infill panel; RC-TP Conf.2, retrofit configuration with a 100 mm thick CLT infill panel; RC-TPext, retrofit configuration with a 57 mm thick CLT panel employed as an externally bonded element.

4. Conclusions

This study investigates via numerical modelling the efficiency of two seismic retrofit solutions based on CLT panels for the seismic strengthening of RC-framed structures. A series of cyclic quasi-static experiments on four full-scale RC frames with construction details typical of the 70s were simulated numerically to predict the effects of the proposed retrofit solutions on the lateral in-plane stiffness and strength. The experiments and numerical analyses included tests on a non-retrofitted masonry-infilled frame (employed as a reference specimen) and three frames retrofitted with CLT panels as infills or externally bonded retrofitting elements (i.e., retrofit interventions RC-TP and RC-TPext).

This paper also presents the results from a parallel companion testing campaign aimed at determining the mechanical characteristics of the materials employed for constructing and retrofitting the RC frame specimens. The tests were carried out to acquire data for calibrating the numerical models. Strength tests were performed on samples of steel and concrete used to construct the RC frames, as well as on mortar prisms, solid bricks, and hollow blocks used to build the infill walls. In addition, four small masonry wallettes made of solid bricks were subjected to diagonal compression tests to determine the mechanical properties (strength and stiffness) of the masonry. Finally, the capacity of timber-to-timber and timber-to-concrete connections was determined through pull-out and push-out tests.

The results of these mechanical characterisation tests were used to fine-tune the numerical models previously developed by the authors. The comparison between experimental observations from full-scale cyclic quasi-static tests and numerical analysis results showed that the numerical models could adequately simulate the seismic response of both non-retrofitted and retrofitted RC frames. Moreover, both numerical and experimental results showed significant improvements in the lateral load-bearing capacity of the RC frames thanks to the proposed seismic retrofit solutions.

Acknowledgements

The research work was carried out within the framework of the 2022-2023 ReLUIS-DPC network (Italian University Network of Seismic Engineering Laboratories and Italian Civil Protection Agency). The JRC authors would also like to acknowledge funding from the European Union's Horizon 2020 research and innovation programme under the Marie Skłodowska-Curie grant agreement No 897822 — NOTICE-EUB.

References

ASTM E519/E519M-15 (2020) "Standard test method for diagonal tension (shear) in masonry assemblages", American Society for Testing and Material.

Cristofaro M. T., D'Ambrisi A., De Stefano M., Pucinotti R., & Tanganelli M., 2012. Studio sulla dispersione dei valori di resistenza a compressione del calcestruzzo di edifici esistenti. Il Giornale delle Prove non Distruttive, Monitoraggio, Diagnostica, 2, 32-39 (in Italian).

Crowley H., Despotaki V., Silva V., Dabbeek J., et al., 2021. Model of seismic design lateral force levels for the existing reinforced concrete European building stock. Bulletin of Earthquake Engineering, 19(7), 2839-2865.

Demirel I. O., Yakut A., Binici B., 2022. Seismic performance of mid-rise reinforced concrete buildings in Izmir Bayrakli after the 2020 Samos earthquake. Engineering Failure Analysis, 137, 106277.

Gaetani d'Aragona M., Polese M., Di Ludovico M., Prota A., 2018. Seismic vulnerability for RC infilled frames: Simplified evaluation for as-built and retrofitted building typologies. Buildings, 8(10), 137.

Hashemi S. A., 2007. Seismic evaluation of reinforced concrete buildings including effects of masonry infill walls. University of California, Berkeley.

Ricci P., Verderame G. M., & Manfredi G., 2011. Analisi statistica delle proprietà meccaniche degli acciai da cemento armato utilizzati tra il 1950 e il 1980. XIV Convegno ANIDIS L'Ingegneria Sismica in Italia, 18-22 (in Italian).

Sezen H., Whittaker A. S., Elwood K. J., & Mosalam K. M., 2003. Performance of reinforced concrete buildings during the August 17, 1999 Kocaeli, Turkey earthquake, and seismic design and construction practise in Turkey. Engineering Structures, 25(1), 103-114.

Smiroldo F., Giongo I., Piazza M., 2021. Use of timber panels to reduce the seismic vulnerability of concrete frame structures. Engineering Structures, 244, 112797.

Smiroldo F., Giongo I., Piazza M., 2020. Seismic retrofit of masonry infilled frames by using timber panels. In 17th World Conference on Earthquake Engineering, 17WCEE 2020, Sendai, Japan.

Smiroldo F., Viel D., Giongo I., Piazza M., 2021. A numerical study on a timber-based retrofit intervention for masonry infilled concrefe frames. In 8th ECCOMAS Thematic Conference on Computational Methods in Structural Dynamics and Earthquake Engineering, COMPDYN 2021, Athens, Greece.

Smiroldo F., Paviani I., Giongo I., Zanon S., Albatici R., Piazza M., 2021. An integrated approach to improve seismic and energetic behaviour of RC framed buildings using timber panels. Sustainability. 2021; 13(20) , 11304.

Eurocode 2: Design of Concrete Structure-part 1-1: general rules and rules for buildings. EN 1992-1-1:2003, Brussels.

Eurocode 6: Design of Masonry Structures-part 1-1: common rules for reinforced and unreinforced masonry structures. EN 1996-1-1:2005, Brussels.

UNI EN 1015-11 (2019) "Methods of test for mortar for masonry – Part 11: Determination of flexural and compressive strength of hardened mortar", European Committee for Standardization.

UNI EN 12504-1 (2021) "Testing concrete in structures – Part 1: Cored specimens – Taking, examining and testing in compression", European Committee for Standardization.

UNI EN 12504-2 (2021) "Testing concrete in structures – Part 2: Non-destructive testing – Determination of rebound number", European Committee for Standardization.

UNI EN 15630-1 (2019) "Steel for the reinforcement and prestressing of concrete – Tests methods – Part 1: Reinforcing bars, rods and wire", European Committee for Standardization.

UNI EN 26891 (1991) "Timber structures – Joints made with mechanical fasteners – General principles for the determination of strength and deformation characteristics", European Committee for Standardization.

UNI EN 772-1 (2015) "Methods of test for masonry units – Part 1: Determination of compressive strength", European Committee for Standardization.

Verderame G. M., De Luca F., Ricci P., Manfredi G., 2011. Preliminary analysis of a soft-storey mechanism after the 2009 L'Aquila earthquake. Earthquake Engineering & Structural Dynamics, 40(8), 925-944.